Detecting signatures of past pathogen selection on human HLA loci: are there needles in the haystack? - Supplementary Figures

Figure S1: Age distribution of the simulated population. This histogram illustrates the numbers of individuals in different age classes at a time point at the end of the simulation in Fig 2. As noted in the Methods, we selected a birth rate parameter and a random background death rate parameter in order to achieve a population age distribution which was plausible for a human population in the absence of modern medical advances – i.e. biased towards younger age classes.

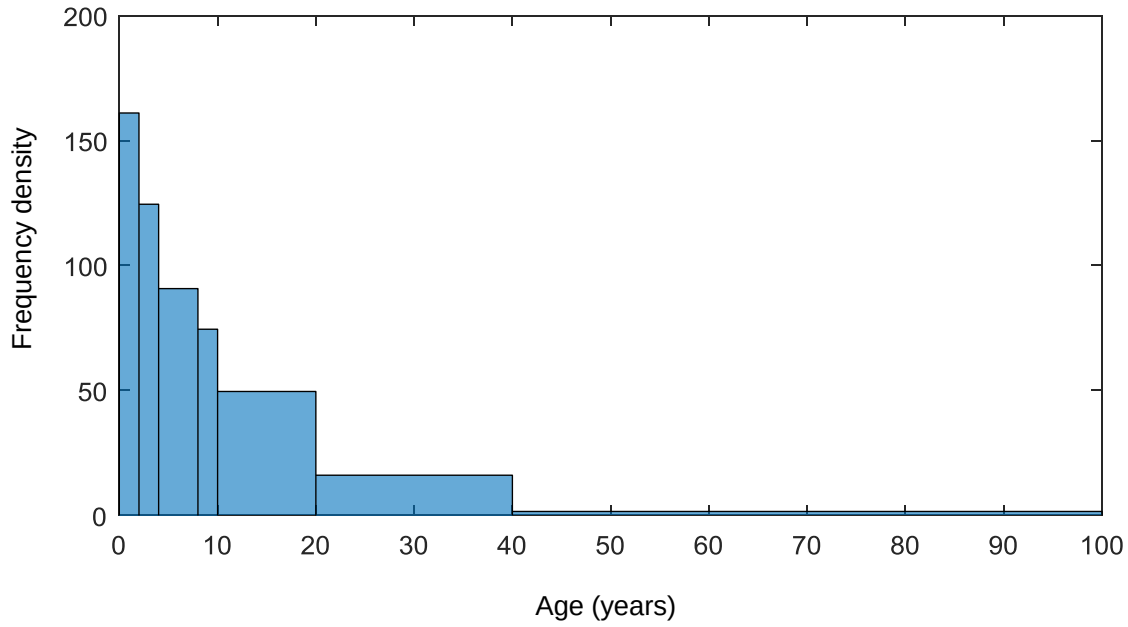

Figure S2: The adaptation of populations under continuous selection from pathogens 1 and 2, with a 1% recombination rate between host HLA loci. The bar chart on the left hand side of each panel illustrates the proportion of simulated populations surviving, out of [tbc] simulations at each parameter combination. The bar chart on the right hand side of each panel illustrates the proportion of the surviving populations displaying adaptation to one or other pathogen, or no adaptation signal (see legend, and see text for definition of different types of adaptation). Within each graph the mortality caused by pathogen 2 (θ_2) increases along the x axis. The mortality caused by pathogen 1 is zero in panel A ($\theta_1 = 0$), and increases in value in panels B and C (B: $\theta_1 = 0.00005$, C: $\theta_1 = 0.0001$). Pathogen 2 has a higher probability of causing death during infection than pathogen 1 ($\theta_2 > \theta_1$) in the regions to the right hand side of the vertical red line in each panel. $\beta_2 = 0.3$, $\sigma_2 = 0.02$ and r =0.01. All other parameter values were as detailed in the Methods.

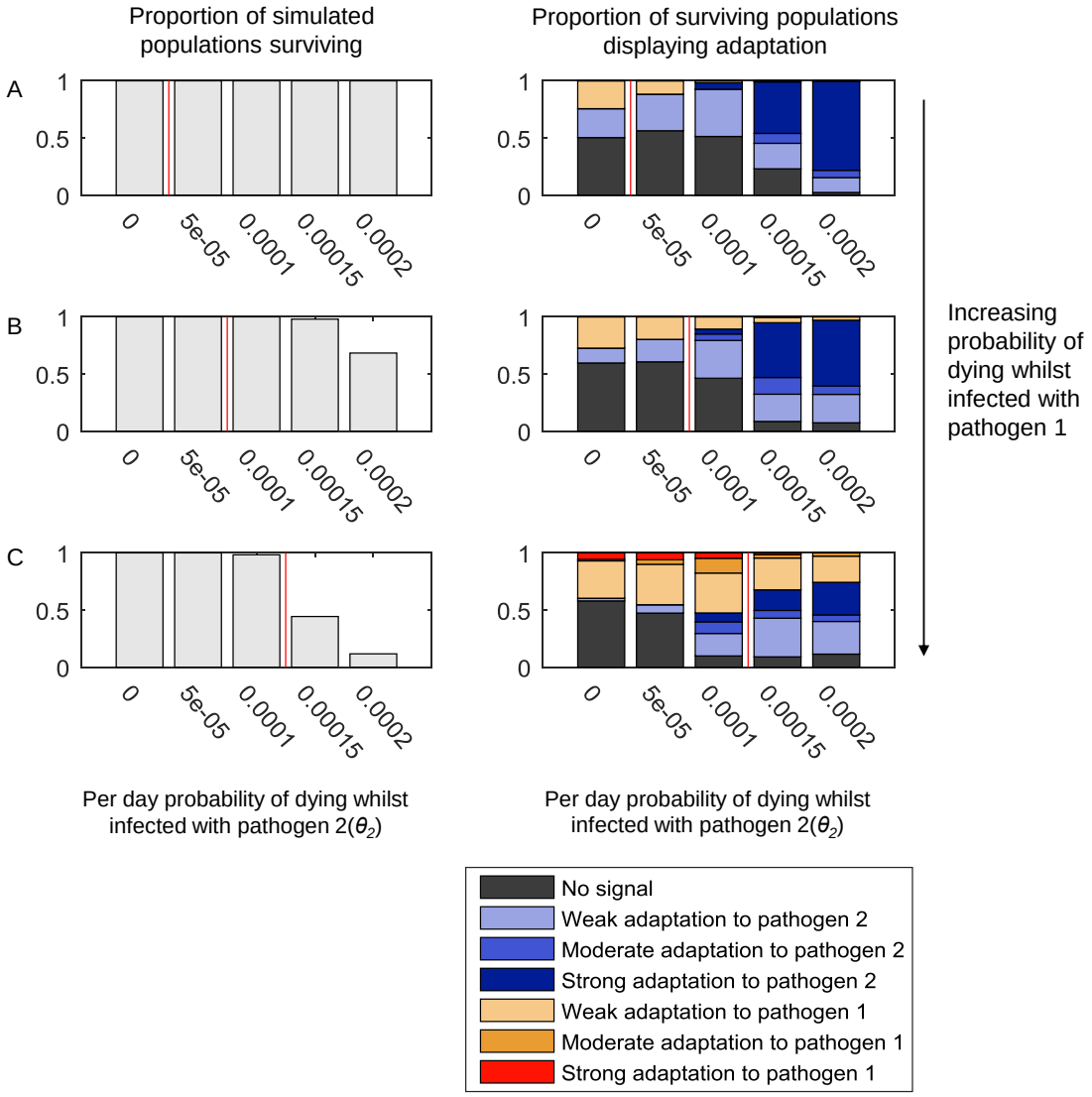

Figure S3: The adaptation of populations under continuous selection from pathogens 1 and 2, with a 5% recombination rate between host HLA loci. The bar chart on the left hand side of each panel illustrates the proportion of simulated populations surviving, out of [tbc] simulations at each parameter combination. The bar chart on the right hand side of each panel illustrates the proportion of the surviving populations displaying adaptation to one or other pathogen, or no adaptation signal (see legend, and see text for definition of different types of adaptation). Within each graph the mortality caused by pathogen 2 (θ_2) increases along the x axis. The mortality caused by pathogen 1 is zero in panel A ($\theta_1 = 0$), and increases in value in panels B and C (B: $\theta_1 = 0.00005$, C: $\theta_1 = 0.0001$). Pathogen 2 has a higher probability of causing death during infection than pathogen 1 ($\theta_2 > \theta_1$) in the regions to the right hand side of the vertical red line in each panel. $\beta_2 = 0.3$, $\sigma_2 = 0.02$ and r =0.05. All other parameter values were as detailed in the Methods.

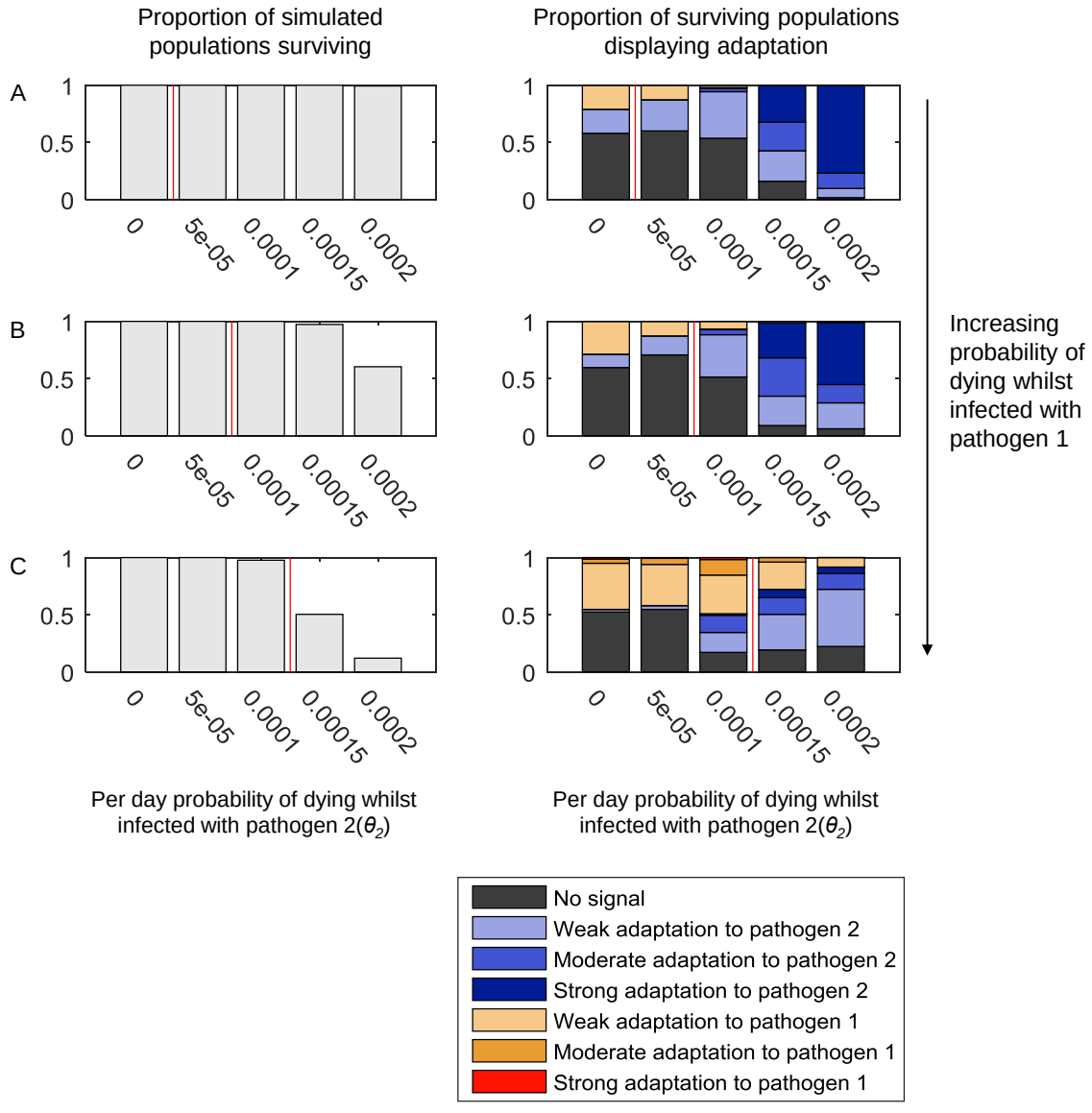

Figure S4: The adaptation of populations under continuous selection from pathogens 1 and 2, where infectious disease mortality is limited to individuals <5 years of age. The bar chart on the left hand side of each panel illustrates the proportion of simulated populations surviving, out of [tbc] simulations at each parameter combination. The bar chart on the right hand side of each panel illustrates the proportion of the surviving populations displaying adaptation to one or other pathogen, or no adaptation signal (see legend, and see text for definition of different types of adaptation). Within each graph the mortality caused by pathogen 2 (θ_2) increases along the x axis. In panel A the per day probability of death whilst infected with pathogen 1 (θ_1) = 0. In panel B, the per day probability of death whilst infected with pathogen 1 (θ_1) = 0.0005. Pathogen 2 has a higher probability of causing death during infection than pathogen 1 ($\theta_2 > \theta_1$) in the regions to the right hand side of the vertical red line in each panel. β_2= 0.3, σ_2 = 0.02 and r =0.01. All other parameter values were as detailed in the Methods.

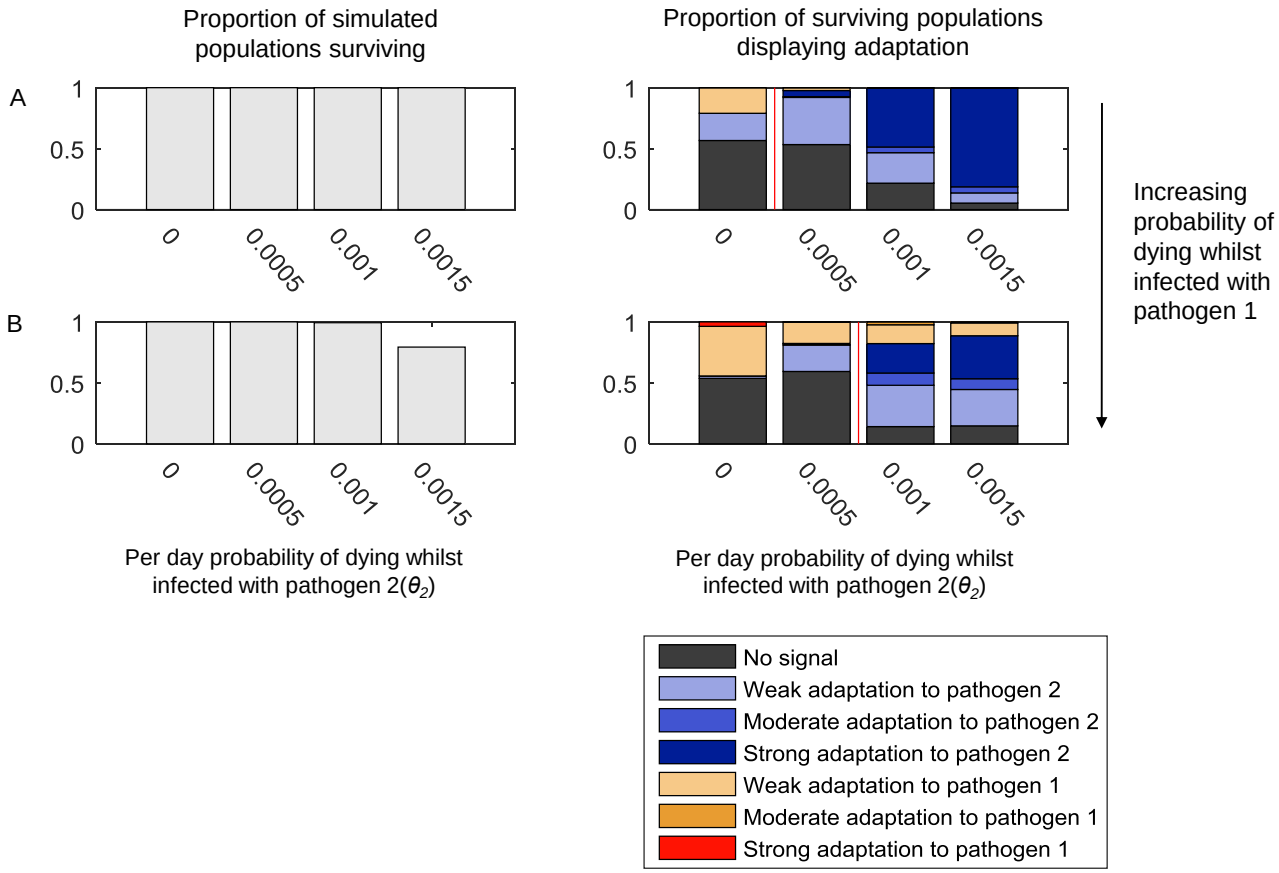

Figure S5: The adaptation of populations under continuous selection from pathogen 1 and intermittent selection from pathogen 2, with a 1% recombination rate between host HLA loci. This figure uses the same layout as figure S2. Unlike in figure S2, however, the transmission parameter and recovery rate for pathogen 2 have been given values that lead to pathogen 2 being lost and re introduced into the population (β_2= 0.4 and σ_2 =0.1). The range of mortality rates affecting to those infected with pathogen 2 (θ_2) are also higher than in figure S2, as indicated by the x axis of each graph. Just as in figure S2, the mortality caused by pathogen 1 is zero in panel A (θ_1 = 0), and increases in value in panels B and C (B: θ_1 = 0.00005, C: θ_1 = 0.0001). r= 0.01, and all other parameters are as given in the Methods.

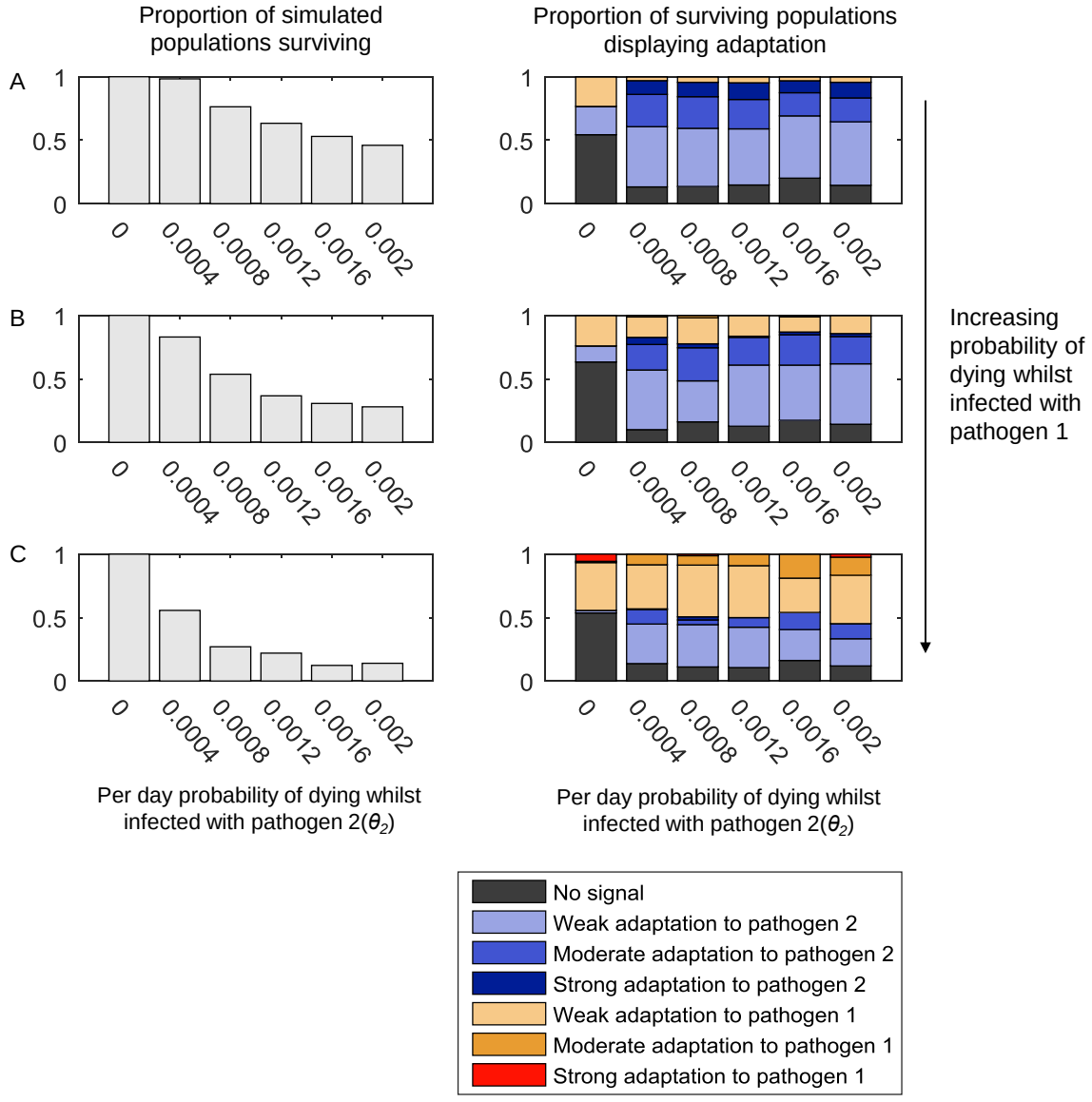

Figure S6: The adaptation of populations under continuous selection from pathogen 1 and intermittent selection from pathogen 2, with a 5% recombination rate between host HLA loci. This figure uses the same layout as figure S2. Unlike in figure S2, however, the transmission parameter and recovery rate for pathogen 2 have been given values that lead to pathogen 2 being lost and re introduced into the population (β_2= 0.4 and σ_2 =0.1). The range of mortality rates affecting to those infected with pathogen 2 (θ_2) are also higher than in figure S2, as indicated by the x axis of each graph. Just as in figure S2, the mortality caused by pathogen 1 is zero in panel A (θ_1 = 0), and increases in value in panels B and C (B: θ_1 = 0.00005, C: θ_1 = 0.0001). r= 0.05, and all other parameters are as given in the Methods.